Structural Flexibility Influence on Vehicle Dynamics Using ADAMS/FEA

D. Kmiec Ford AVT-CSI J. McConville MDI

Body and frame structural compliance has long been suspected of contributing to the vehicle dynamics performance of passenger cars and light trucks. A method now exists to quantify the effects of vehicle structural compliance on handling response by combining traditional finite element methods with ADAMS large displacement capabilities. With these two analytical methods combined to form ADAMS/FEA, it is now possible to identify compliance sources, their effects on vehicle handling, and develop efficient design modifications to reduce or eliminate the unwanted compliance.

This paper will review efforts made to analyze a rear wheel drive, body-on-frame (BOF) passenger car vehicle dynamics characteristics with and without structural compliance. Three model configurations were used to identify compliance effects; rigid, rigid with body mounts, and compliant frame with mounts. Each model is run through an identical handling maneuver using a closed-loop driver model to eliminate analysis variability. Results are reduced, filtered and plotted for interpretation. A design modification is then made to the vehicle frame to investigate an intuitive source of structural compliance that influenced transient handling behavior. A visual method to identify compliance sources is discussed. This method will enable an analyst to magnify the structural deformation and animate with the non-flexible model components.

Body on Frame (BOF) Vehicle Description

As a result of initial driver perceptions of prototype vehicle handling, it was felt that the flexibility of the vehicle frame, in conjunction with the cushioning due to body/frame elastomeric isolation, might be adversely effecting the Body on Frame (BOF) Vehicle handling performance under certain maneuvers. To examine this possibility, it was proposed to enhance the existing BOF Vehicle (ref. Fig. 1) handling model to see if this suspicion was analytically founded. To this end, a functional BOF Vehicle handling model was developed with the task of making the following modifications and enhancements;

>Tire algorithms to be converted to the latest Ford vehicle dynamics methodology

>Tire test data for the Michelin tires (@ 32psi) to be reduced into splines and incorporated into model

>Incorporation of closed loop driver to permit the ADAMS model to follow a pre-determined ground path

>The ADAMS model lumped body/frame/powertrain to be separated into individual components and re-connected using appropriate linear and non-linear bushings and mounts

>The BOF Vehicle 50,000+ grid NASTRAN frame model to be appropriately condensed using ADAMS/FEA(Discrete) and incorporated into the ADAMS model

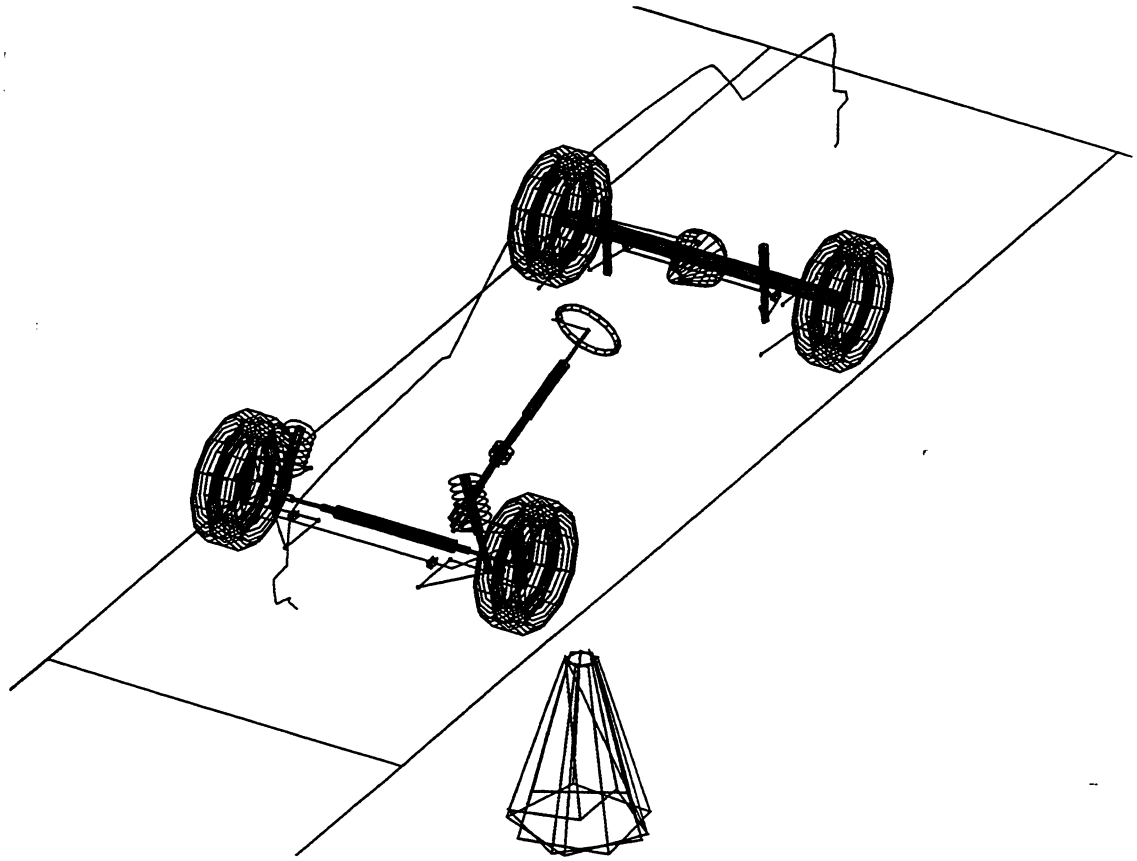

Fig. 1 Initial BOF Vehicle Handling Model

In addition, because this effort is to serve as a guideline for future reference, it was required to maintain three, parallel, ADAMS maneuvering models;

1) bofr.adm-------Rigid frame, rigid body ---rigid connection,
2) bof.adm--------Rigid frame, rigid body ---bushed connection,
3) boff.adm-------Flex frame, rigid body -----bushed connection.

With the exception of the flexible modeling of the vehicle frame, most of the revisions to the maneuvering models were simple applications of already-existing FORTRAN subroutines and standard ADAMS modeling entities.

Conversion of BOF Vehicle NASTRAN Frame Model

Fig. (2) shows the NASTRAN model of the BOF Vehicle frame.

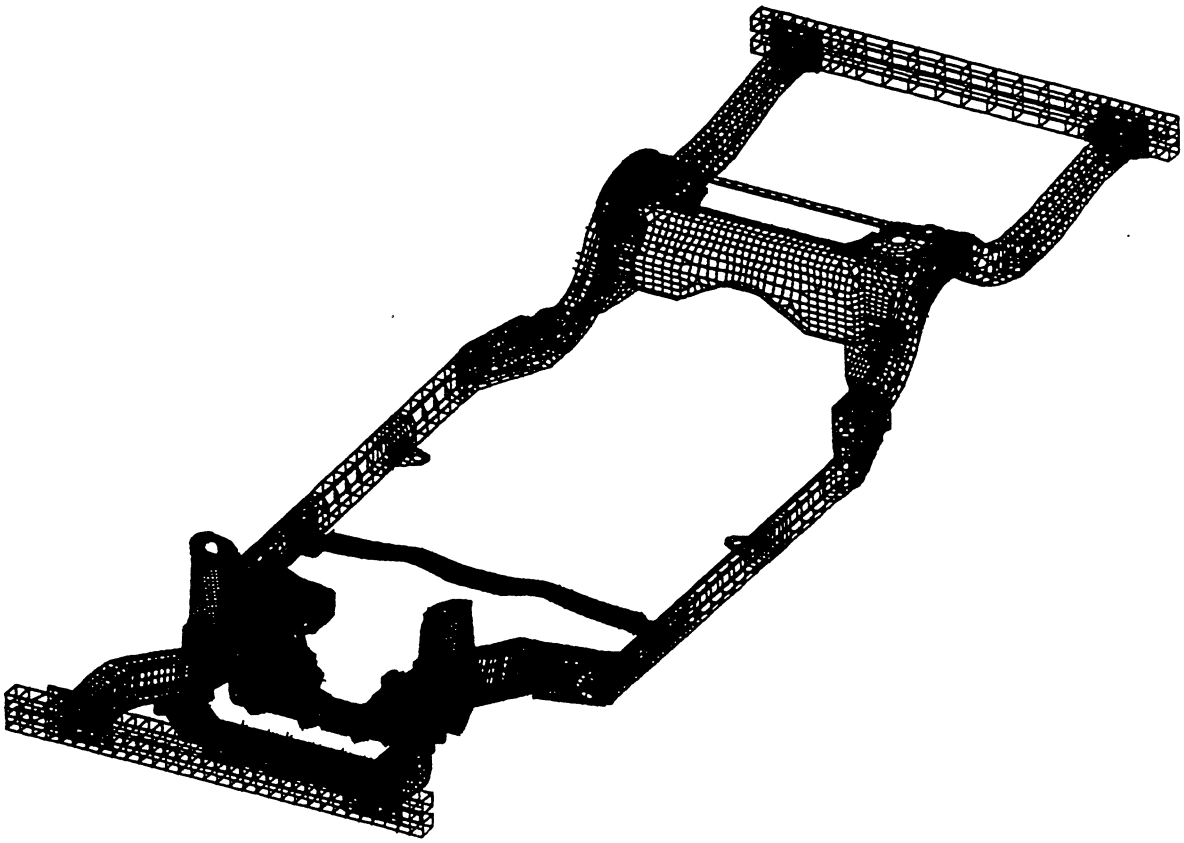

Fig. 2 BOF Vehicle NASTRAN Model

Because of its great size, the BOF Vehicle frame model posed some special problems for condensation via ADAMS/FEA(Discrete), and the same methods were employed as were reported in [1]. While the number of 'hard points'. i.e., points where other components (chassis and body) are attached is 45 and, thus, within the ADAMS/FEA(Discrete) program limit of 50, the number of grids and elements far exceeds the default array size limits of ADAMS/FEA(Discrete) used for geometric data storage. While these defaults are capable of being increased, it was opted to make a minimal-geometry 'surrogate' frame (ref. Appendix A) comprised of simple NASTRAN CBAR elements and having as NASTRAN GRIDs only those points selected as 'exterior' (e.g. 'master' nodes) for the condensed model. A list of these retained, 'hardpoint' locations is given in Table 1 below.

Table 1 -- BOF Vehicle Frame Model Structural Hardpoints

NASTRAN GRID ID		X	Y	Z	HARDPOINT IDENTIFICATION
GRID	1	983.549	000.0000	693.6000	(dummy interior point)
GRID	1453	983.549	-574.9800	693.6000	bushing F (front lft)
GRID	2244	983.5498	574.9800	693.6000	bushing F (rgt)
GRID	3886	1515.540	-450.9680	936.5900	shock twr (front lft)
GRID	4433	1515.540	450.9699	936.5900	shock twr (front rgt)
GRID	7425	2110.000	-655.0000	506.0000	bushing 1B (lft)
GRID	7426	2085.000	-526.0000	506.0000	bushing 1 (lft)
GRID	7427	2085.000	526.0000	506.0000	bushing 1 (rgt)
GRID	7428	2110.000	655.0000	506.0000	bushing 1B (rgt)
GRID	7489	3189.000	-615.6000	377.3700	bushing 2 (lft)
GRID	7490	3189.000	615.6000	377.3700	bushing 2 (rgt)
GRID	9930	2517.690	+000.0000	451.1000	trans mnt
GRID	13543	5745.698	-558.5000	628.2998	bushing 6 (lft)
GRID	13552	5745.698	558.5000	628.2998	bushing 6 (rgt)
GRID	14220	4684.198	-507.8990	769.5000	bushing 4 (rgt)
GRID	14221	4586.578	-450.3700	772.0000	spring seat (rr lft)
GRID	14359	4432.109	-447.350	757.5299	shock seat (rr lft)
GRID	14690	4432.109	447.3500	757.5299	shock seat (rr rgt)
GRID	14828	4586.578	450.3700	772.0000	spring seat (rr rgt)
GRID	14829	4684.198	507.8999	769.5000	bushing 4 (rgt)
GRID	15729	4334.040	-502.2790	487.0699	stabar atbofh (rr lft)
GRID	15932	4334.040	502.2799	487.0699	stabar atbofh (rr rgt)
GRID	17088	5078.198	-617.0000	574.0000	bushing 5 (lft)
GRID	17188	3972.73	-580.21	471.0	bushing 3 (lft)
GRID	17854	5078.198	617.0000	574.0000	bushing 5 (rgt)
GRID	17949	3972.730	580.2100	471.0000	bushing 3 (rgt)
GRID	18434	4417.238	-490.5400	526.3300	latrl link (rr lft)
GRID	18435	4478.979	509.1800	612.2500	latrl link (rr rgt)
GRID	38172	1541.999	-370.0000	393.9997	aarm atbofh (fr lft lowr aft)
GRID	38177	1541.999	369.9999	393.9997	aarm atbofh (fr rgt lowr aft)
GRID	45097	4104.163	-638.3920	394.3565	drag link (rr lft lwr)
GRID	45098	4379.95	-618.68	585.96	drag link (rr lft uppr)
GRID	45100	4103.561	638.3457	395.2195	drag link (rr rgt lwr)
GRID	45102	4379.952	618.6784	585.9623	drag link (rr rgt uppr)
GRID	45103	1388.500	-470.0000	661.0000	aarm atbofh (fr lft uppr fwd)
GRID	45104	1634.000	-470.0000	616.0000	aarm atbofh (fr lft uppr aft)
GRID	45105	1230.000	-370.0000	394.0000	aarm atbofh (fr lft lowr fwd)
GRID	45107	1648.000	-411.0000	404.0000	strg atbofh #1-#2
GRID	45112	1388.500	470.0000	661.5000	aarm atbofh (fr rgt uppr fwd)
GRID	45113	1634.000	470.0000	616.0000	aarm atbofh (fr rgt uppr aft)

GRID	45114	1230.000	370.0000	394.0000	aarm attch (fr rgt lowr fwd)
GRID	45118	1298.073	429.7762	469.0265	stabar attch (fr rgt)
GRID	45121	1298.074	-429.9350	469.0267	stabar attch (fr lft)
GRID	45124	1648.038	205.4490	403.9982	strg attch #3
GRID	45125	1658.090	-183.5000	591.6000	engine mnt (lft)
GRID	45126	1658.300	+208.4000	593.6000	engine mnt (rgt)

When executed on NASTRAN, this model results in a more manageably-sized NASTRAN .PCH file. Standard UNIX editing is then employed to remove the fictitious mass and stiffness data from this file and replace it with the valid mass and stiffness data removed from the .PCH file of the full model run on Ford's CRAY C90. This (edited) .PCH file is then run through the ADAMS/FEA NASUNI and UNIADM modules [2] to create a 'data set fragment', i.e., an ADAMS file containing only those PARTs, MARKERs, FORCEs and GRAPHICs relating to the frame component. Fig. 3 shows the condensed frame model (data set 'fragment') resulting from the process.

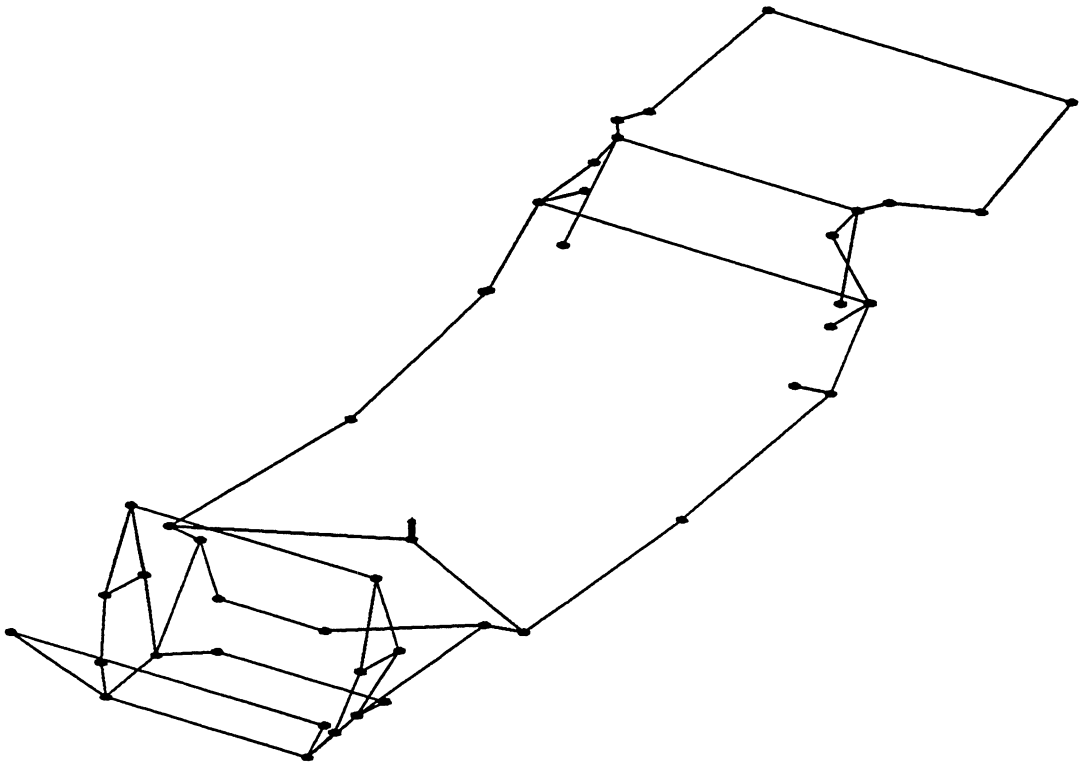

Fig. 3 Reduced Frame Model

Next, a copy is made of the ADAMS BOF Vehicle model with the rigid frame and the fragment is edited onto the bottom of it, after which the PART entries for the rigid frame are removed from the model and any of their entries associated with other system components or forces are re-assigned to the nearest, appropriate elastic (sub)PART of the compliant frame. A new ADAMS PART now exists for each master GRID. ADAMS/FEA(Discrete) 'tags' the new PARTs by embedding the GRID number in the PART name. For example, the part corresponding to GRID 1453 (the front left frame corner) is given below;

```
!              >>>>>>>>>> PART 500001  (G1453) <<<<<<<<<<
!
!                  *** adams_view_name='G1453_PART'
PART/ 500001, MASS=  9.556930E+00, CM= 500001
, IP= 9.556930E+00, 9.556930E+00, 9.556930E+00
, VX=-2.011680E+04
!                  *** adams_view_name='G1453_CM'
MARK/ 500001, PART= 500001                !G145 Center of mass marker.
, QP= 9.835498E+02,-5.749800E+02, 6.936000E+02
!                  *** adams_view_name='G1453_NF'
MARK/ 500002, PART= 500001                !G145 Nforce attachment - ZD
, QP= 9.835498E+02,-5.749800E+02, 6.936000E+02
!                  *** adams_view_name='G1453_GRA'
MARK/ 500003, PART= 500001                !G145 Graphics attachment.
, QP= 9.835498E+02,-5.749800E+02, 6.936000E+02
!                  *** adams_view_name='G1_GRA'
MARK/ 500004, PART= 500001                !G1   Graphics attachment.
, QP= 9.835498E+02, 0.000000E+00, 6.936000E+02
!                  *** adams_view_name='G45105_GRA'
MARK/ 500005, PART= 500001                !G451 Graphics attachment.
, QP= 1.230000E+03,-3.700000E+02, 3.940000E+02
GRAP/ 500001, CIRC, CM= 500001, R=  1.638E+01   !Mass center graphics.
GRAP/ 500002, CI, SE=4, CM= 500001, R=  1.638E+01!Mass center graphics.
GRAP/ 500003,                          !Graphic outline between grids:
, O=500003, 500004                       !1453, 1
GRAP/ 500004,                          !Graphic outline between grids:
, O=500003, 500005                       !1453, 45105
```

Model Validation

Prior to any substantial dynamic analysis of the flexible model, it is desirable to verify that the flexible components have been properly condensed and, further, that they have been properly incorporated into the rest of the vehicle model. To accomplish this, a free-free modal analysis was done on the condensed frame model, and a quasi static suspension analysis was done on a full vehicle model employing the flexible frame.

a)Modal Verification of Condensed BOF Vehicle Frame Model

The ADAMS/FEA(Discrete)-condensed frame was subjected to an ADAMS/Linear analysis [3]. Fig. 4 compares the first frame structural mode (torsion) from laboratory test data with

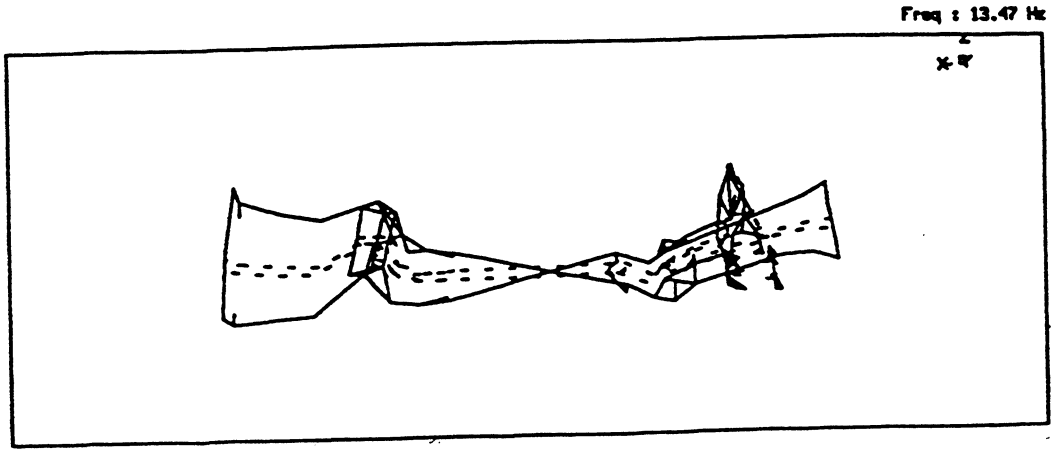

Test

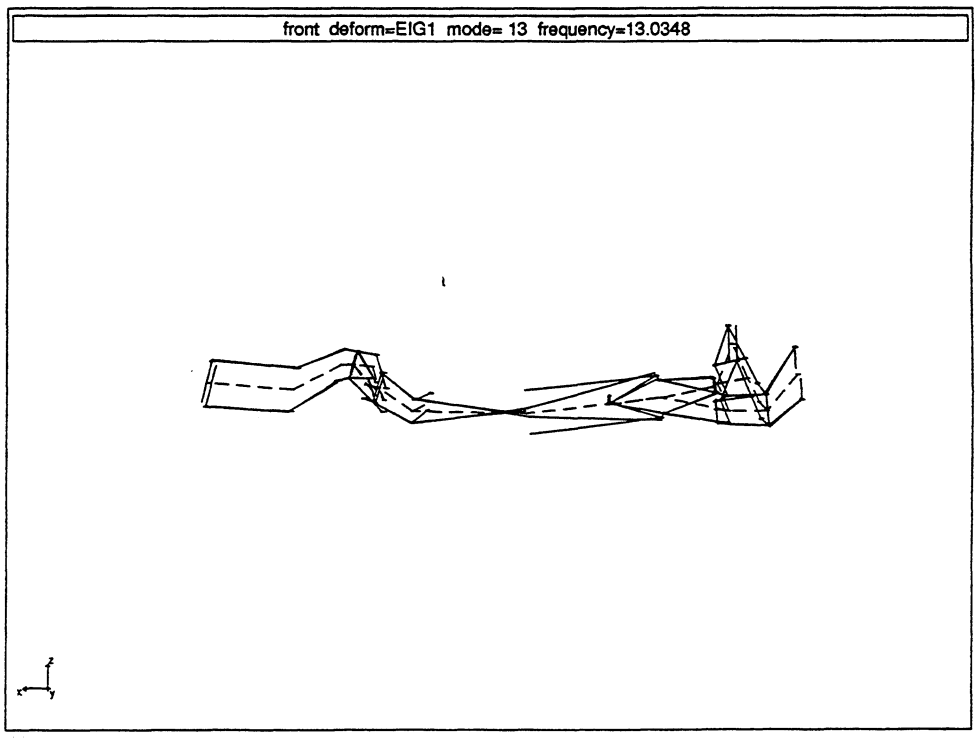

ADAMS/LINEAR

Fig. 4 BOF Vehicle Frame Mode Test vs. ADAMS/Linear

the corresponding analytical results on the condensed frame. A table of mode frequency correlation (hz) for the first 9 test modes is given below:

Mode #	Mode Description	test fq	ADAMS
1	1st Order Torsion	13.47	13.03
2	1st Order Bending	14.06	16.14
3	1st Order Lateral Bending	18.11	18.99
4	2nd Order Lateral Bending & Torsion	25.16	26.15
5	2nd Order Bending	34.37	27.30
6	2nd Order Torsion & Lateral Bending	37.47	37.18
7	#3 Crossmember Vertical Bending	43.51	45.54
8	#3 Crossmember Longitudinal Bending	48.56	49.92
9	3rd Order Torsion and Lateral Bending	51.41	56.54

b)Static Verification of Full BOF Vehicle -- Laboratory Model(s)

The rigid (bof) and flexible (boff) dynamic models were used as a basis for generating ADAMS models of the Laboratory BOF Vehicle front/rear suspension testing. Note that, since the laboratory test grounds the vehicle frame, it was not felt useful to run a bofr version of the test. Changes made to the handling models include:

-addition of 'load pads' at all 4 corners of the vehicle. These are constrained to the wheel at the unloaded tire radius using ATPOINT joint primitives. The pads are also constrained to GROUND using ORIENTATION joint primitives which prevent angular motion of the pads with respect to ground.

-addition of an anchor bushing between ground and the frame, located at the nominal (curb) position of the body CG.

-removal of maneuvering tires and replacement with GFORCES. Note, the tire force is now applied directly to the tire, instead of to the spindles. The GFORCE provides a single vertical restraint to the tire at a rate of 200 N/mm initially. This is used to bring the vehicle into static equilibrium. During this phase, the bushing stiffness vales are limited to reduced (arbitrary) values in the X-, Y-, and AZ- directions.

-the use of DIFFs to trap and maintain the initial vertical static values of the tire forces when the suspension loading in the lateral or fore/aft direction is applied. During this load application, the anchor bushing stiffnesses securing the vehicle to ground are set to a high (arbitrary) value in all directions. For the flexible model, a fictitious 'yoke' is used to distribute the frame anchor loads to the (6) clamp center positions of the test rig. Note that the clamp/frame attachments at these 6 points are assumed rigid.

-special requests are used to compute the wheel center displacements corresponding to the physical test measurements. These results (for both the rigid and flex models) are overplotted onto the test results which have been written into ADAMS/View format from an EXCEL spreadsheet.

Special Note: In all results reported so far, the vehicle body has been assumed rigid. This assumption is based on the comparisons of the trace

of the frame stiffness matrix with the trace of the body stiffness matrix at the same points. In all instances, the stiffnesses for the body exceeded those of the frame by a factor of 10 or more.

Fig. 5 is a photograph of the subject vehicle on the test stand, and fig. 6 Shows the corresponding ADAMS (flexible) model of the BOF Vehicle on the (virtual) test stand.

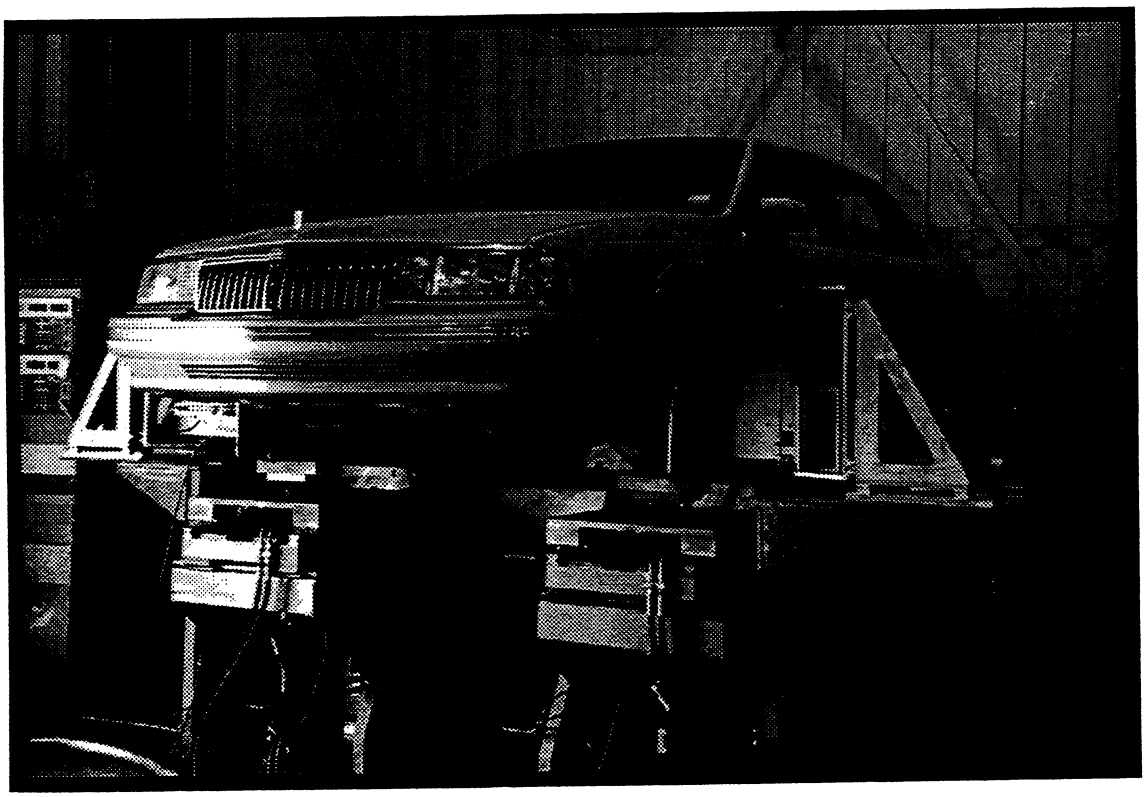

Fig. 5 BOF Vehicle Suspension Test

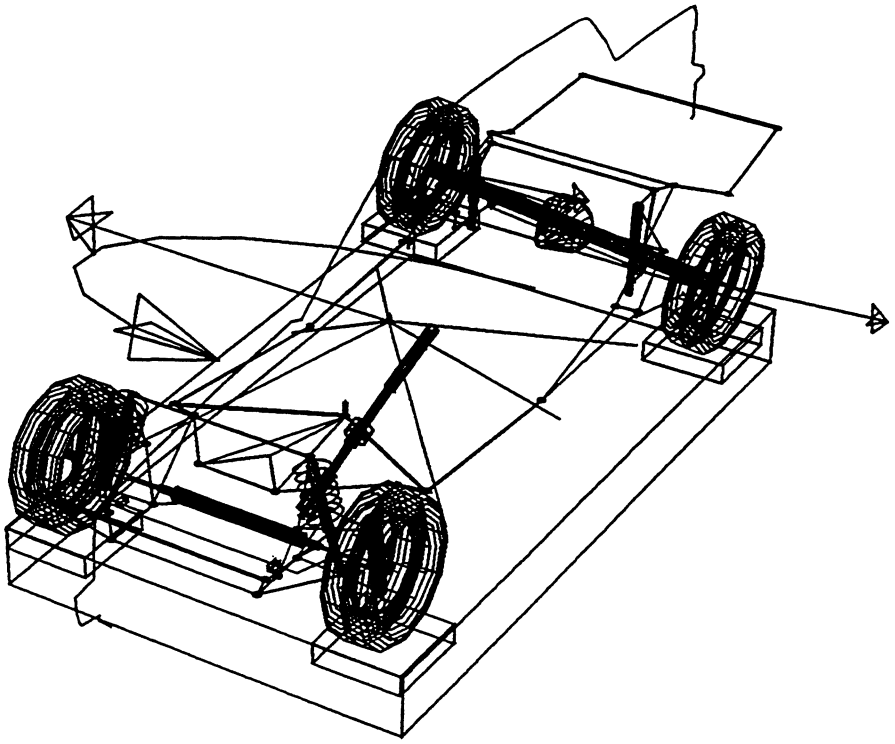

Fig. 6 ADAMS BOF Vehicle Suspension Test Model

Fig. 7 plots the rear wheel lateral deflection due to lateral load for the test vehicle, the rigid model (bushed body/frame), and flex frame models.

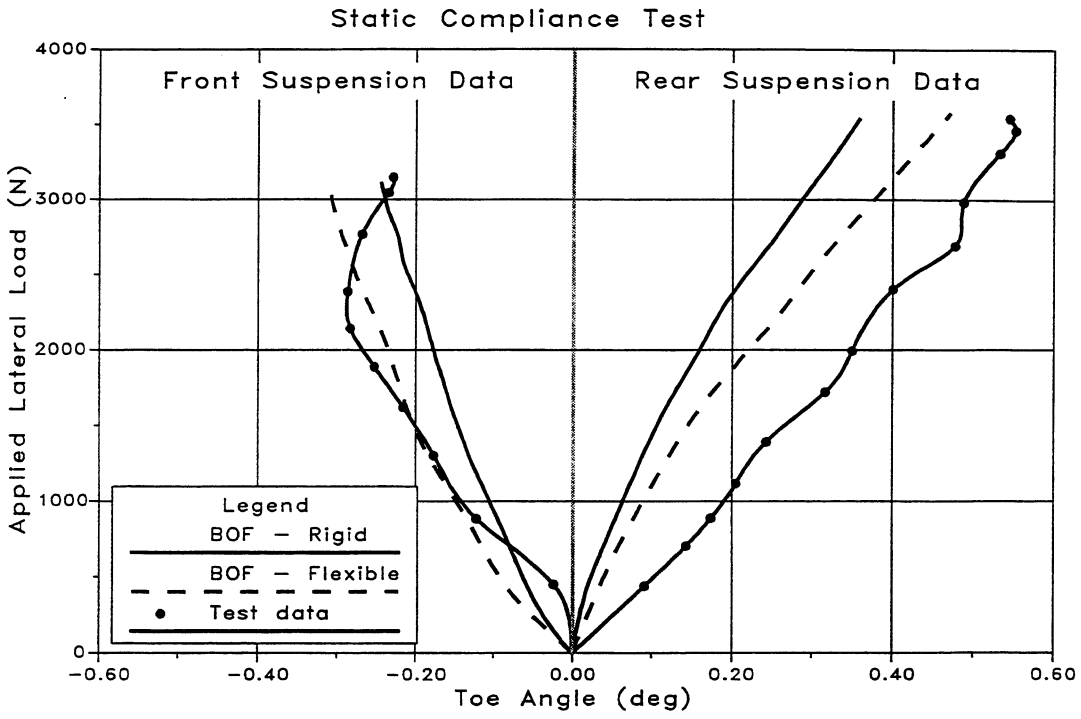

Fig. 7 Laboratory Suspension Test/ADAMS Model Correlation (bof, boff)

Dynamic Simulations--Original Configurations

A) Lane Change Maneuver

The lane change maneuver is accomplished by having the closed-loop controller attempt to match a path in the ground plane specified by an ADAMS SPLINE function. The controller attempts to reduce the separation of a vehicle-fixed reference point from the curve to zero, while simultaneously bringing the vehicle's longitudinal axis tangent to the curve. The severity of the steering maneuver can be controlled by specifying 'gain' values which control the steering motion.

Figures 8 through 11 compare the path, side slip angle, steering wheel angle, and yaw rate for the rigid, bushed, and bushed-flex frame models respectively. Typical run statistics (on an SGI Indy) for these analyses are given below.

Rigid:	Degrees-of-freedom	--> 90
	# of Equations	--> 1605
	% Sparcity	--> 0.576
	CPU Time (sec)	--> 187.0
Bush:	Degrees-of-freedom	--> 102
	# of Equations	--> 1682
	% Sparcity	--> 0.657
	CPU Time (sec)	--> 211.7
Flex:	Degrees-of-freedom	--> 366
	# of Equations	--> 2601
	% Sparcity	--> 3.191
	CPU Time (sec)	--> 4707.9

B) Random Steer Maneuver

The three models were also subjected to a random steer maneuver in which the steering wheel was subjected to an (open-loop) motion as a function of time:. The form of the expression is:

$$\theta(t) = \theta_{max} \bullet \sin(4t^2)$$

For this analysis, the maximum steering angle, θ_{max}, was determined from a continuous turn maneuver in which the steering wheel angle was slowly increased until the desired lateral acceleration was attained. Two lateral acceleration rates, 0.2G and 0.35G were explored.

Figures 12 and 13 compare the lateral acceleration and yaw rate frequency response functions (FRF's) for the three models.

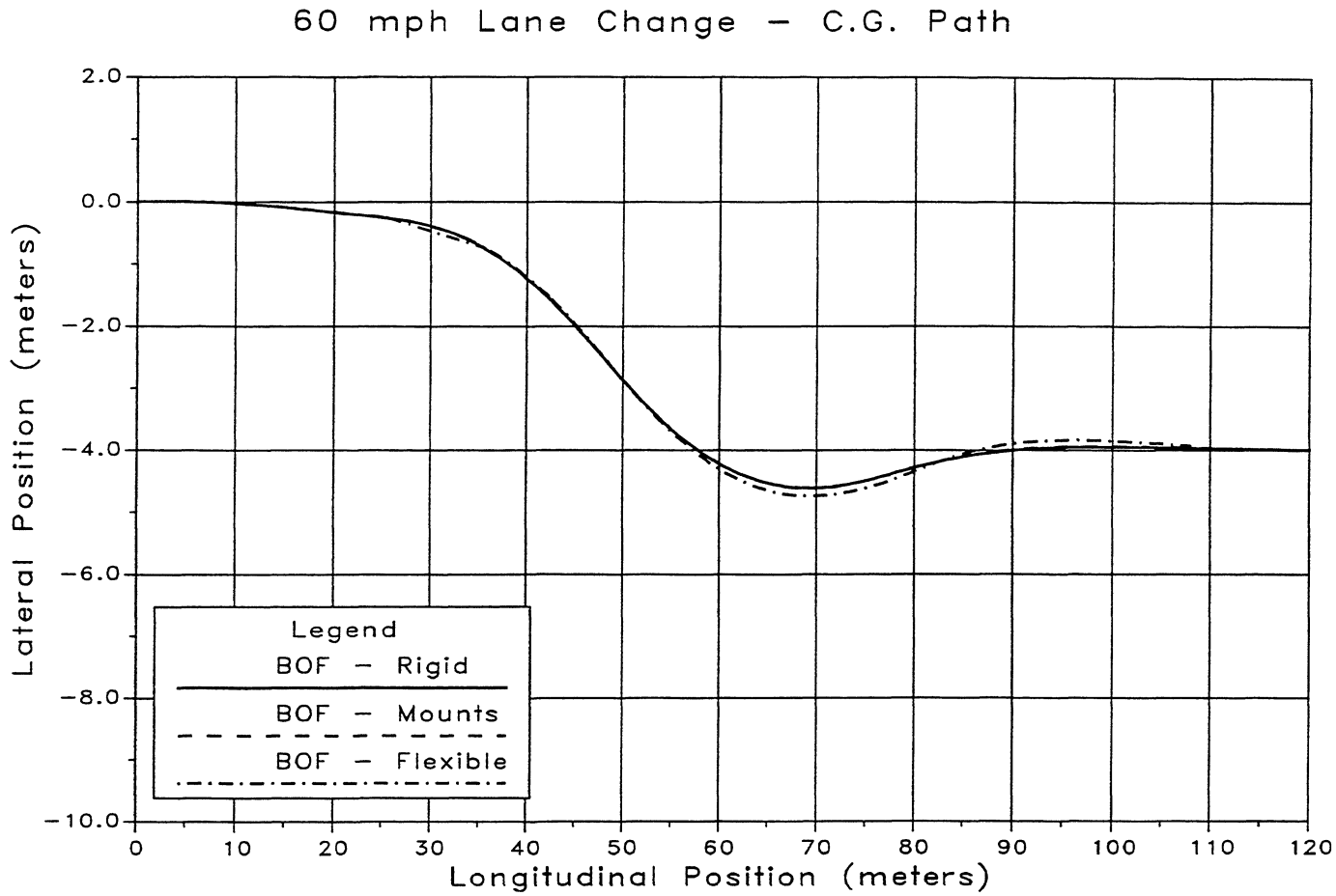

Fig. 8 Lane Change Path Comparison: Rigid, Bushed. Bushed-Flex

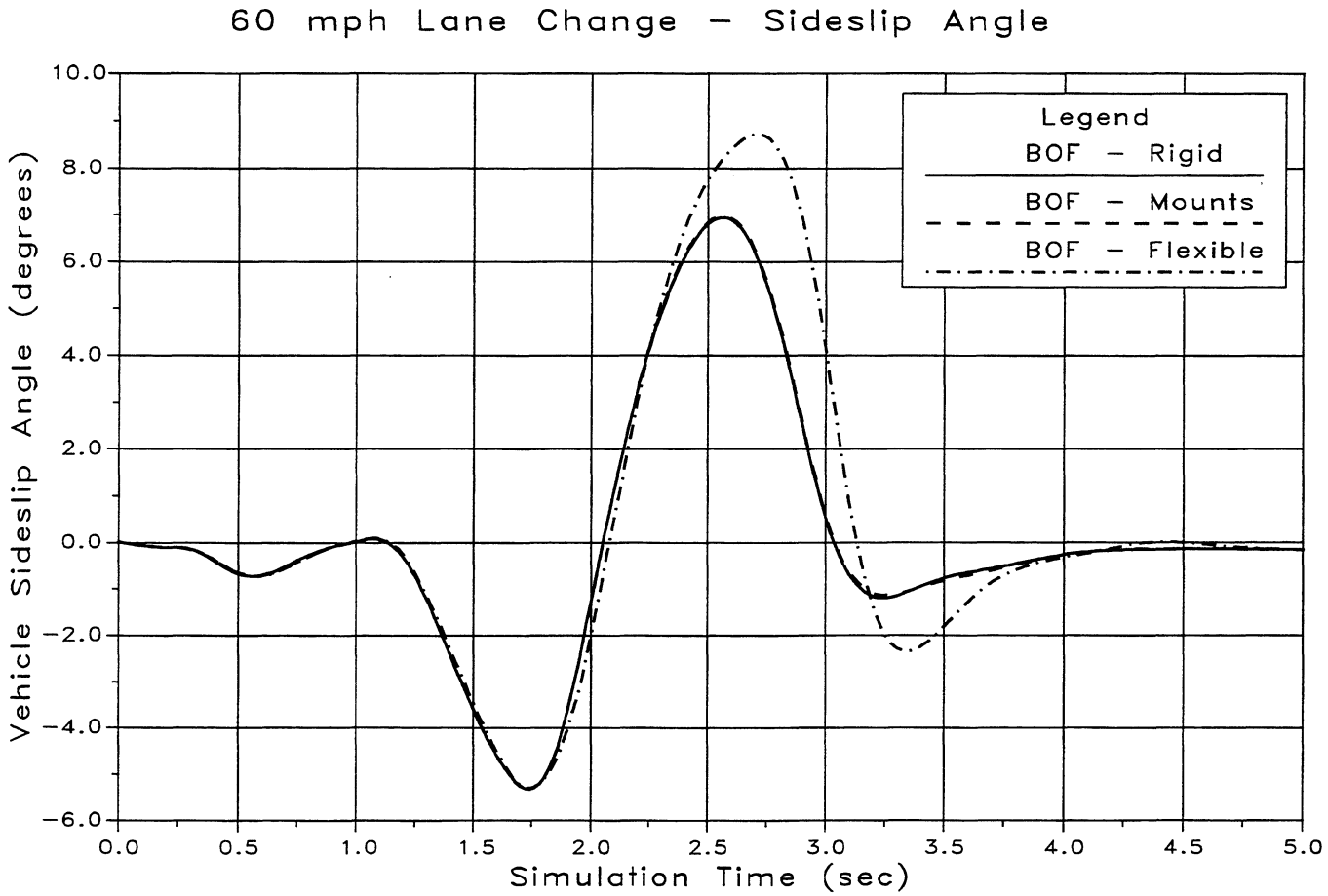

Fig. 9 Lane Change Side Slip Comparison: Rigid, Bushed. Bushed-Flex

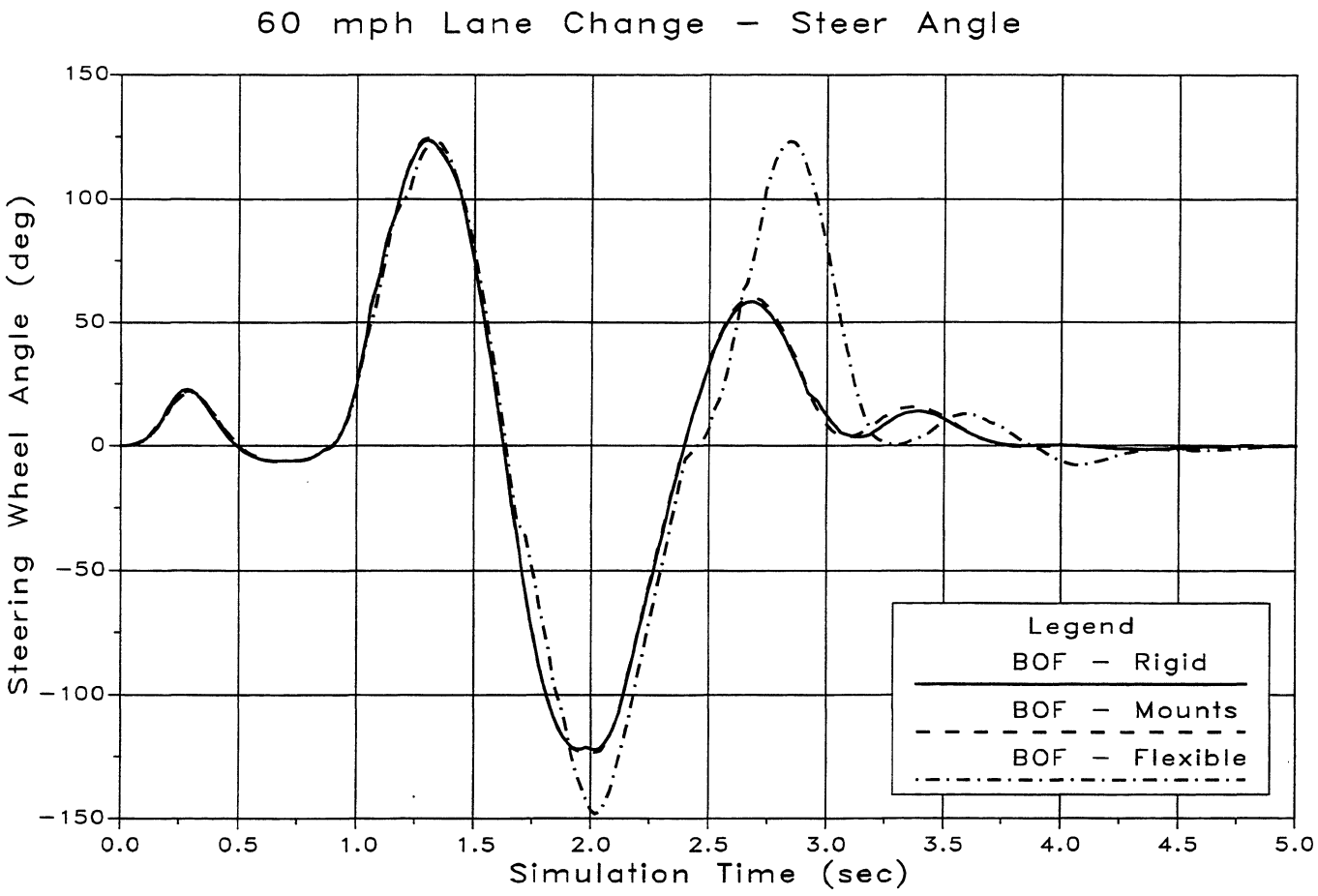

Fig. 10 Lane Change Steering Wheel Angle: Rigid, Bushed. Bushed-Flex

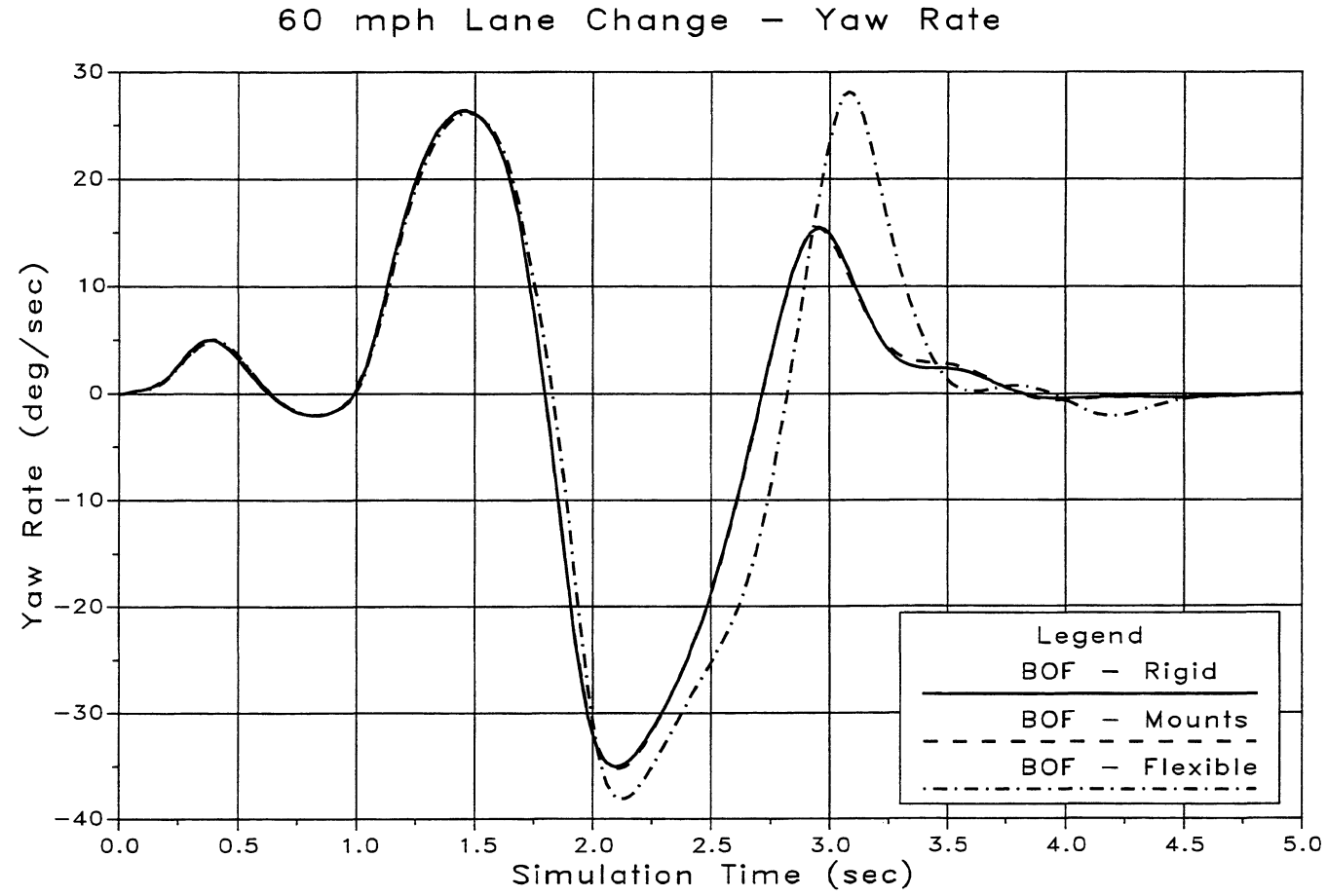

Fig. 11 Lane Change Yaw Rate Comparison: Rigid, Bushed. Bushed-Flex

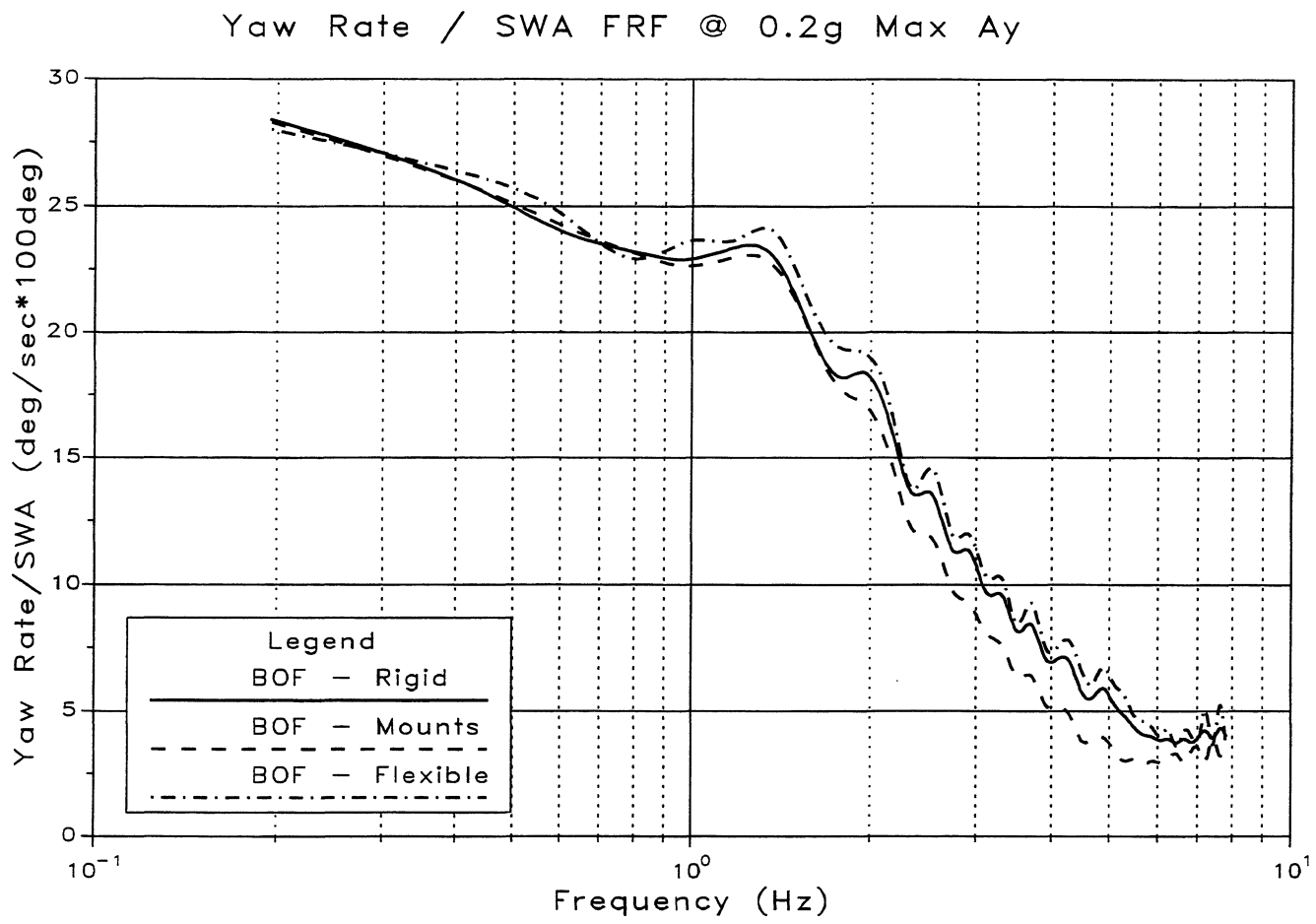

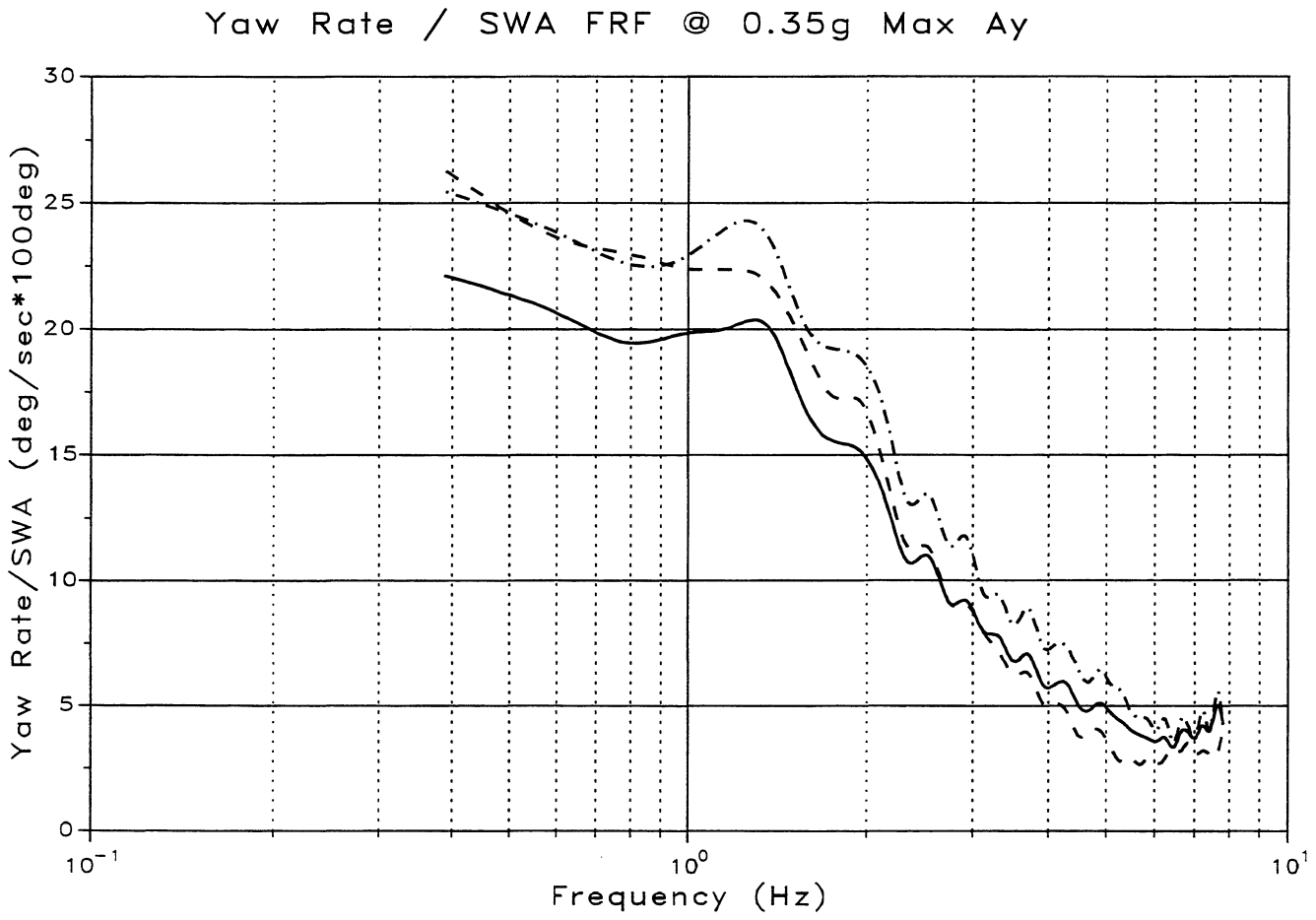

Fig. 12 Yaw FRF Comp: Rigid, Bushed. Bushed-Flex -- at 0.2G & 0.35G

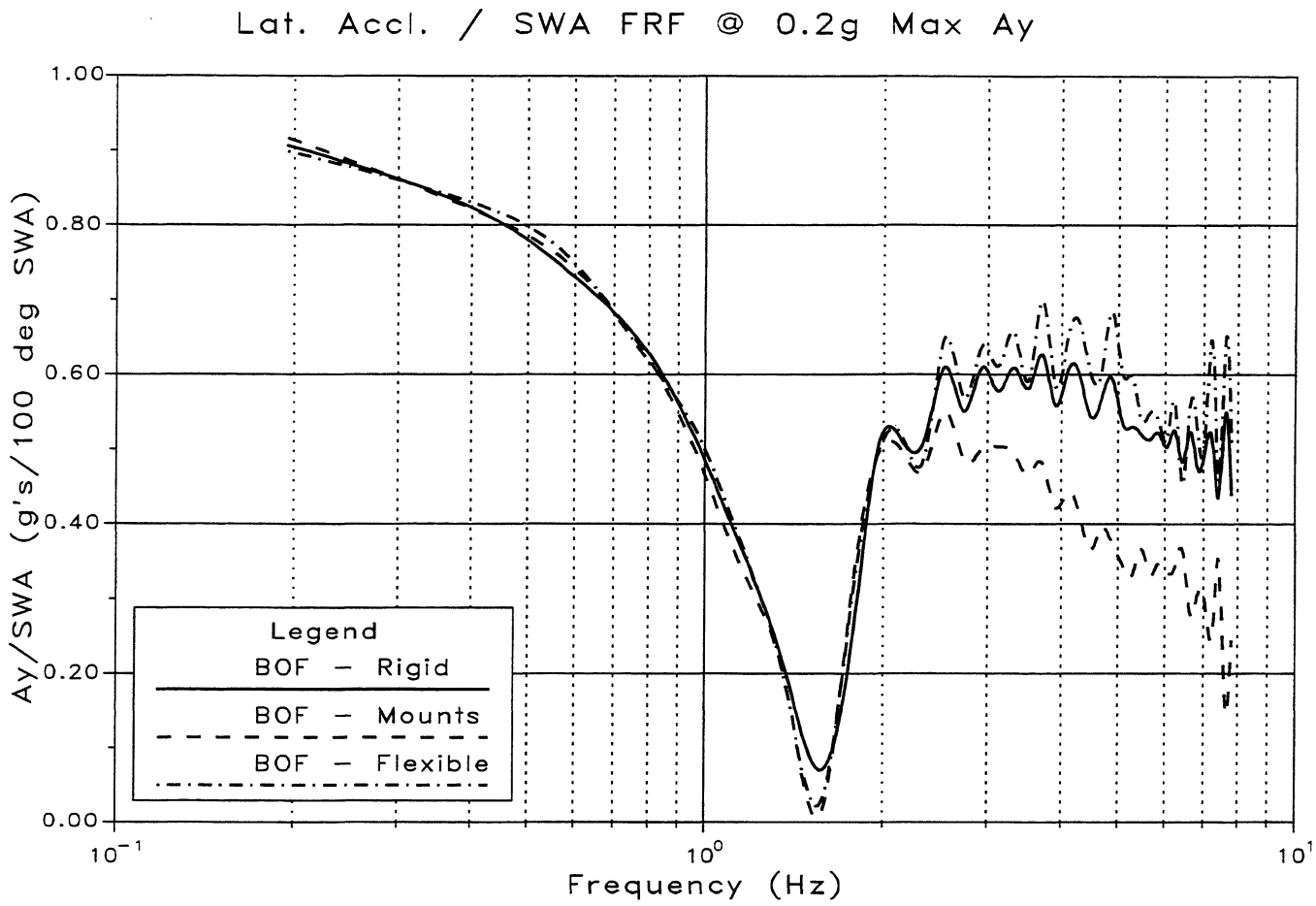

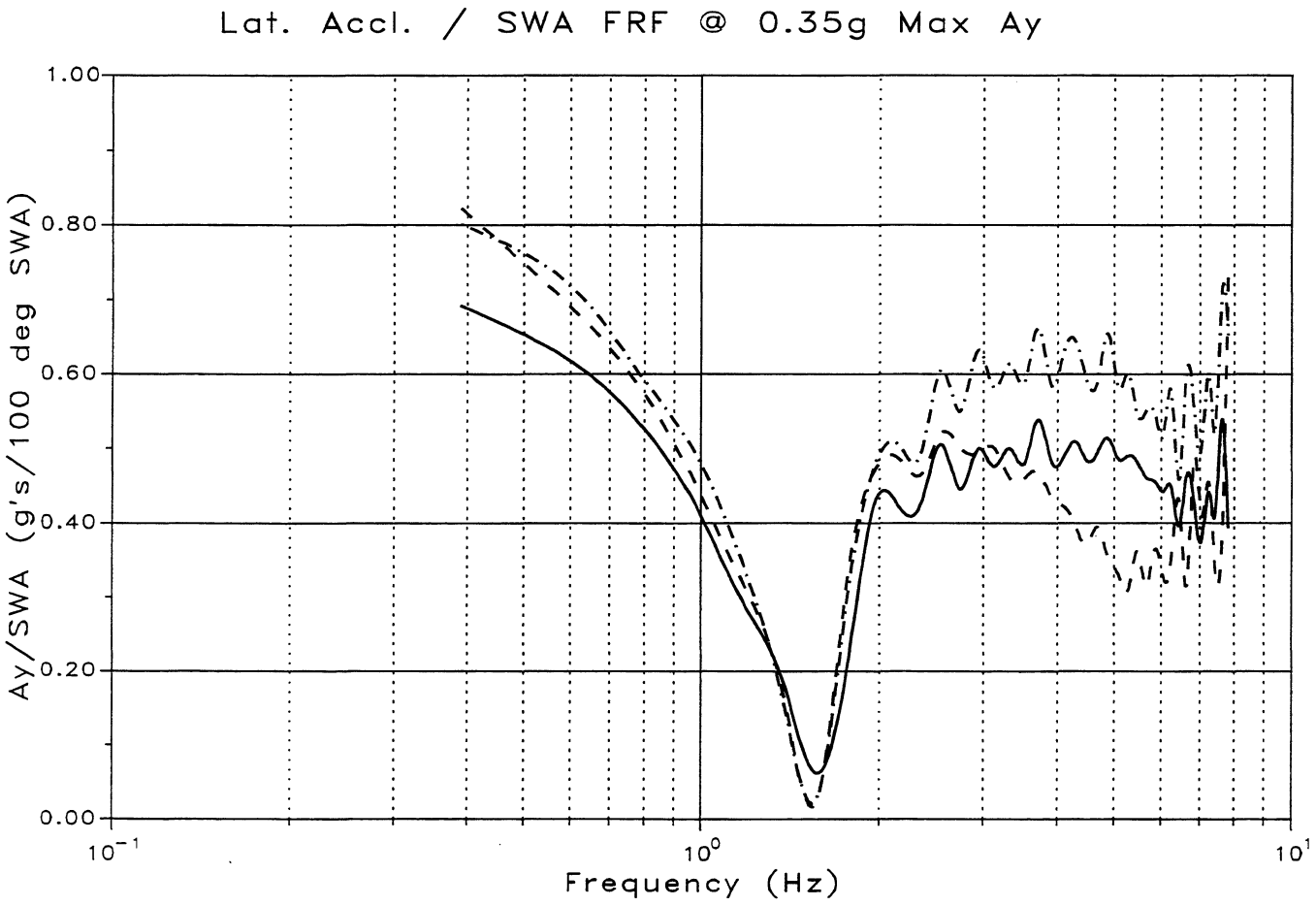

Fig. 13 Lat. Acc.FRF Comp: Rigid, Bushed. Bushed-Flex Flex --at 0.2G & 0.35G

Flexible Frame Modifications

In order to evaluate the effects of stiffening the frame structure without the necessity of extensive and, perhaps, ineffective modifications to the frame NASTRAN model, ADAMS BEAM elements were used to insert an "X-frame" into the existing structure (ref. fig. 14). This structure,

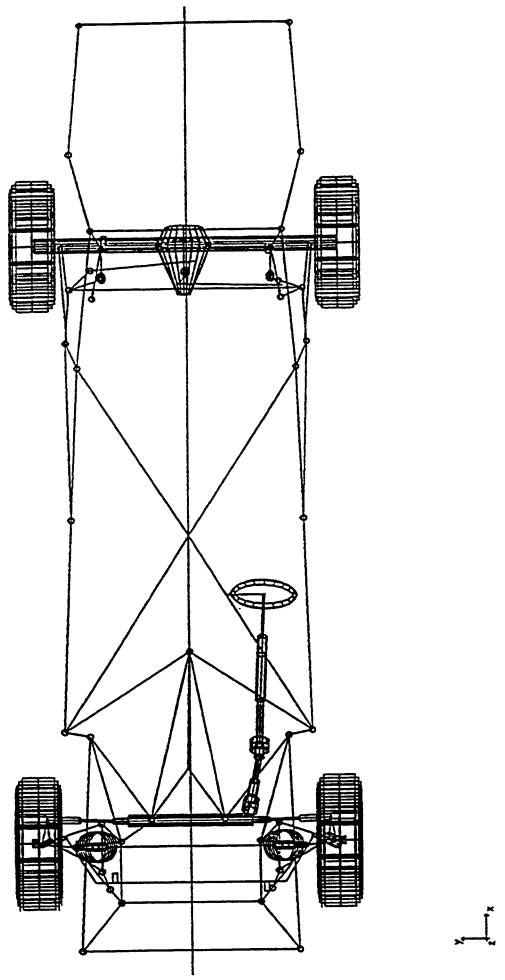

Fig. 14 BOF Stiffened Frame Structure

consisting of 2-inch square (1/8 inch wall thickness) steel tubing, runs from the bushing 1b position on each side to the bushing 3 position on the other side. At their juncture on the centerline, the tubes are joined (e.g., "welded" together). This model was then run through the closed-loop, 12ft (@60mph) lane-change maneuver. Figures 15 and 16 give comparisons between the rigid, flexible frame and X-frame models for yaw rate and steering wheel angle. Figs. 17 and 18 compare the slip angle and tire forces for all the models.

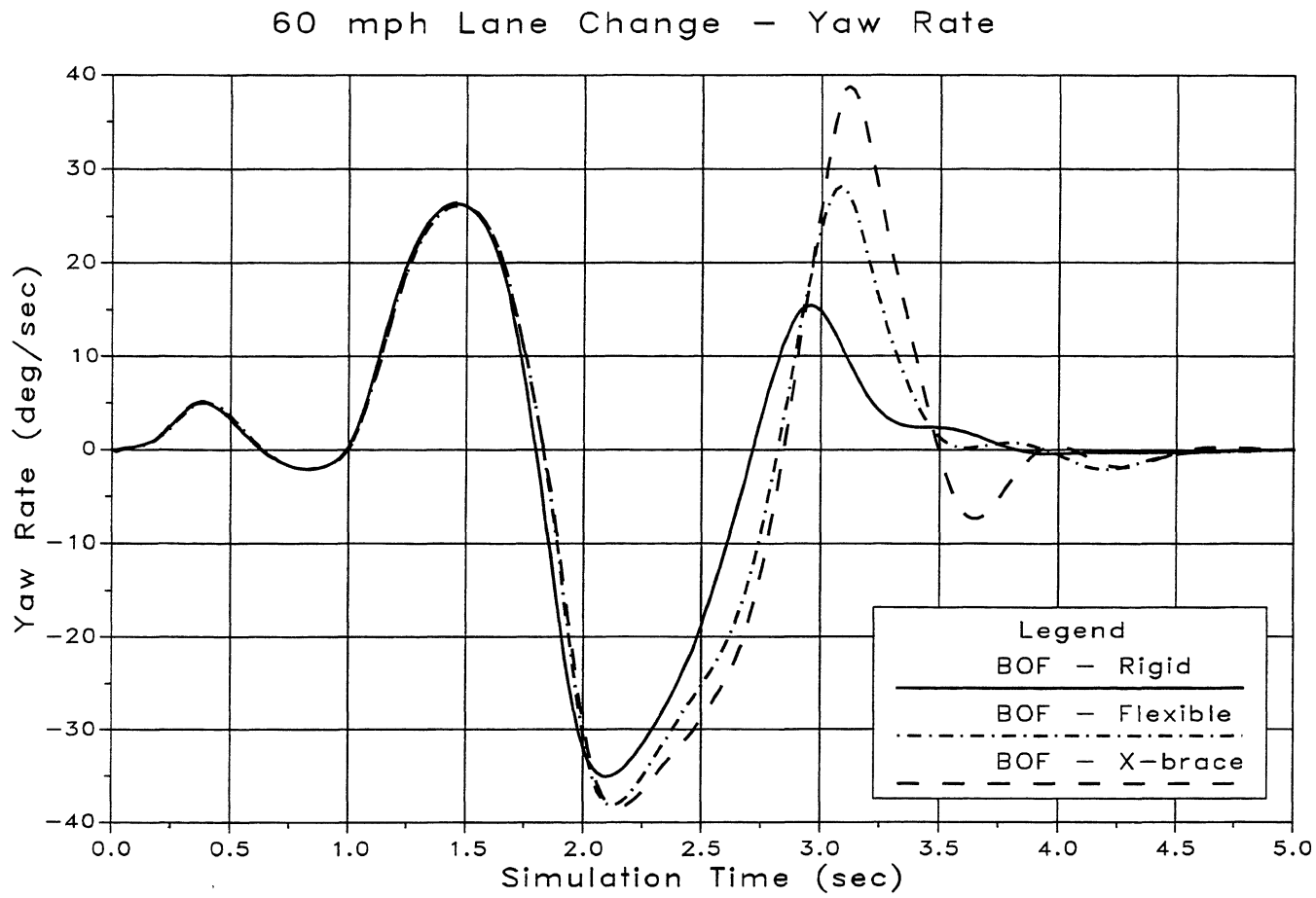

Fig. 15 Lane Change Comparison -- Rigid, Flexible, X-Frame -- Yaw Rate

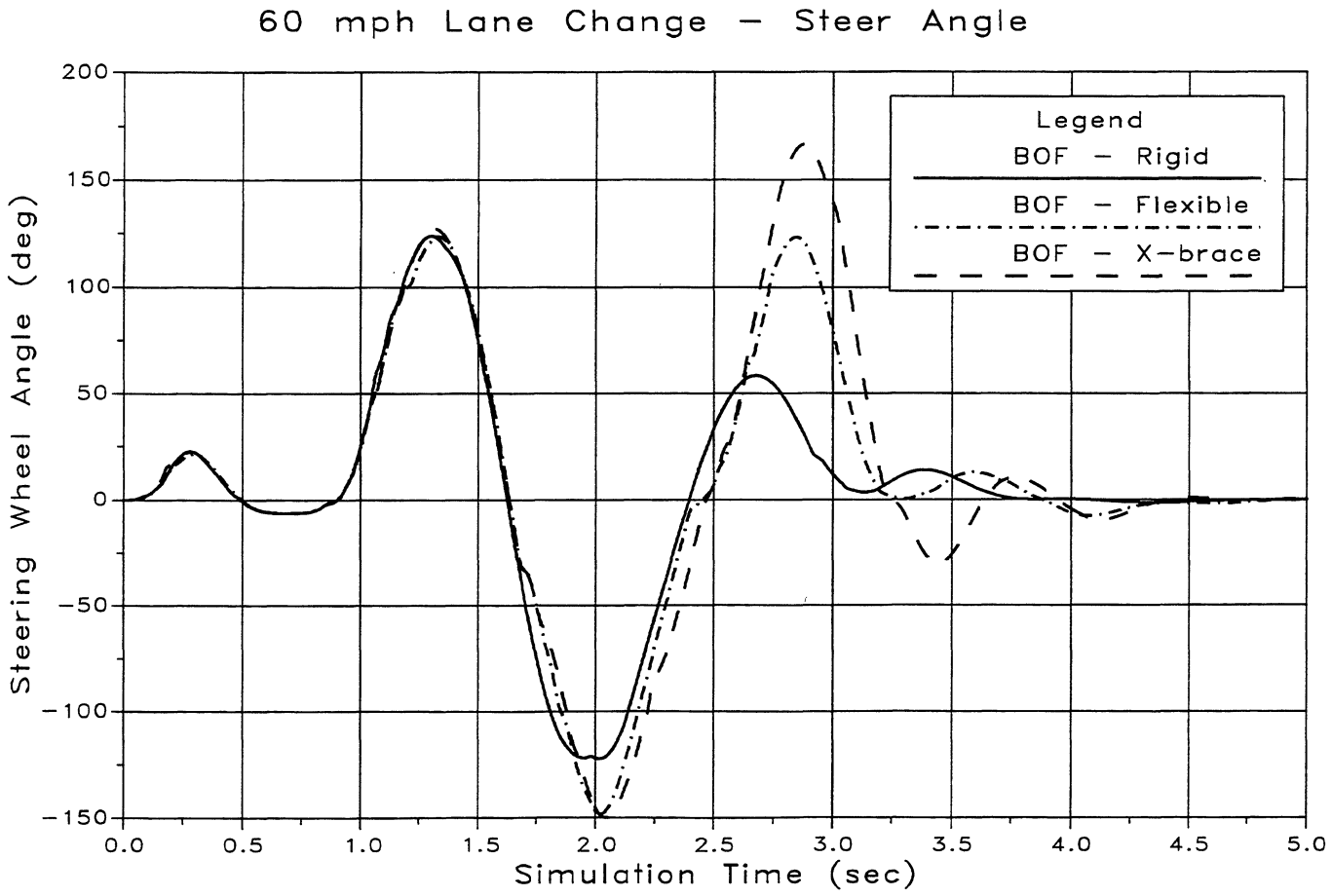

Fig. 16 Lane Change Comparison -- Rigid, Flexible, X-Frame -- Steer Angle

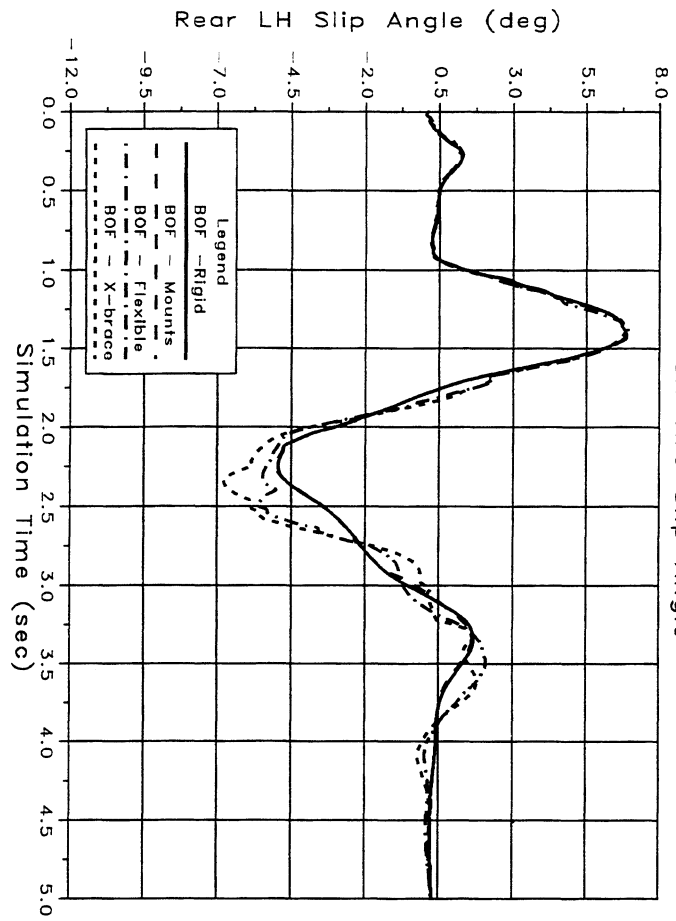

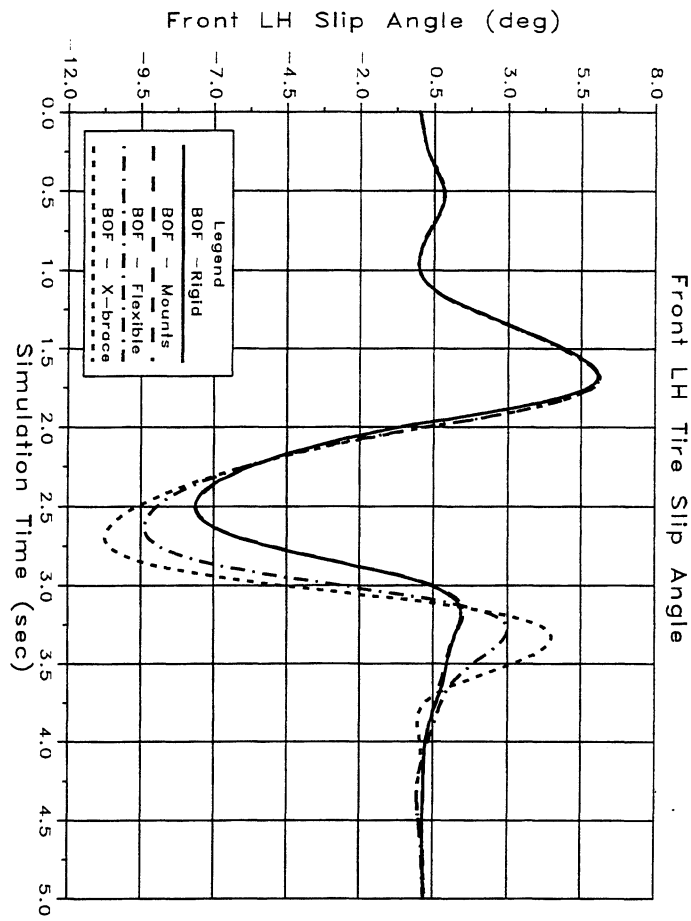

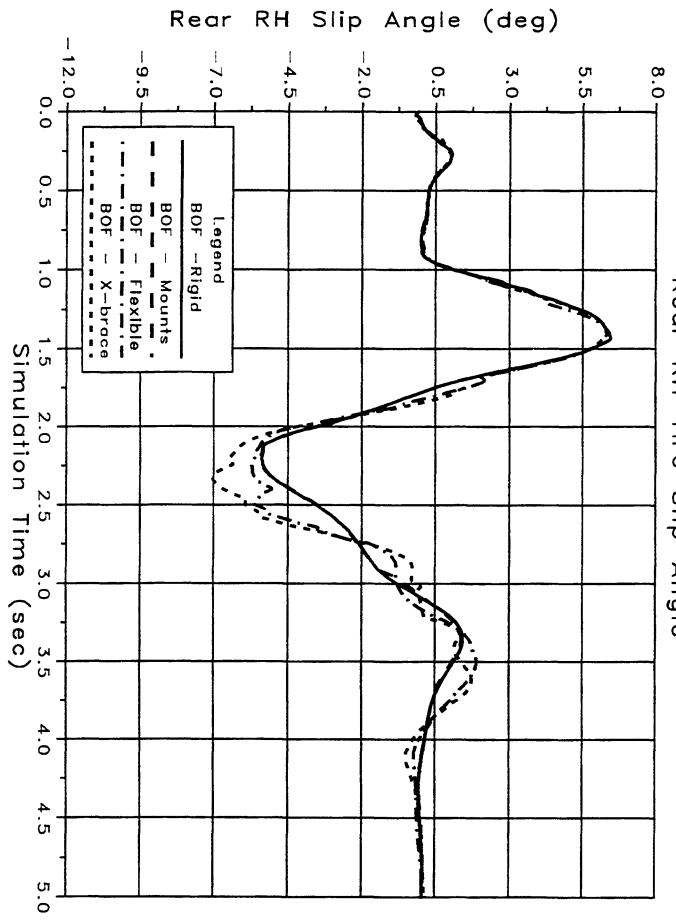

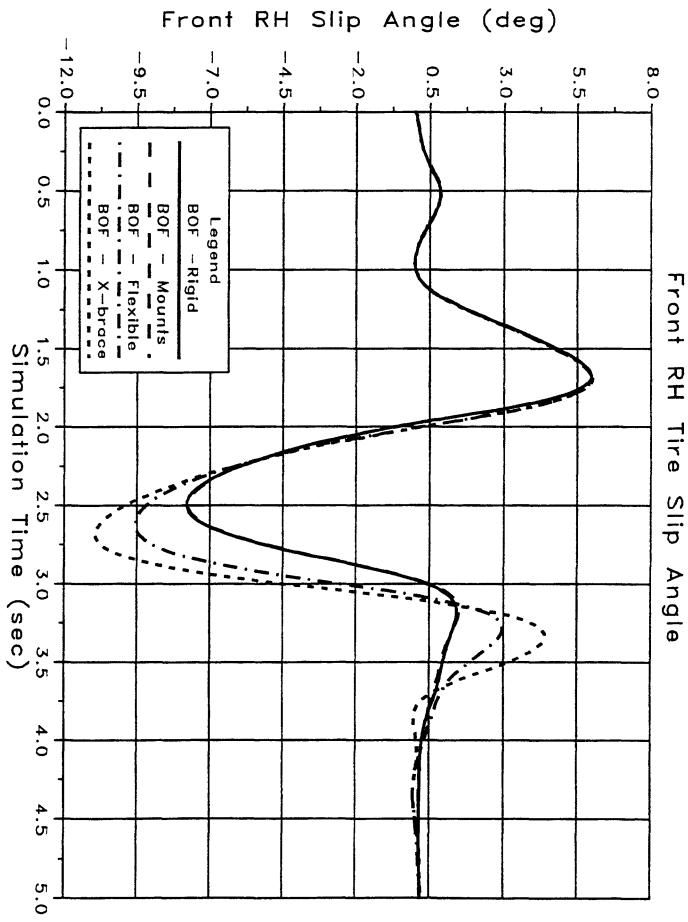

Fig. 17 Lane Change Comparison -- All 4 Models -- Tire Slip Angles

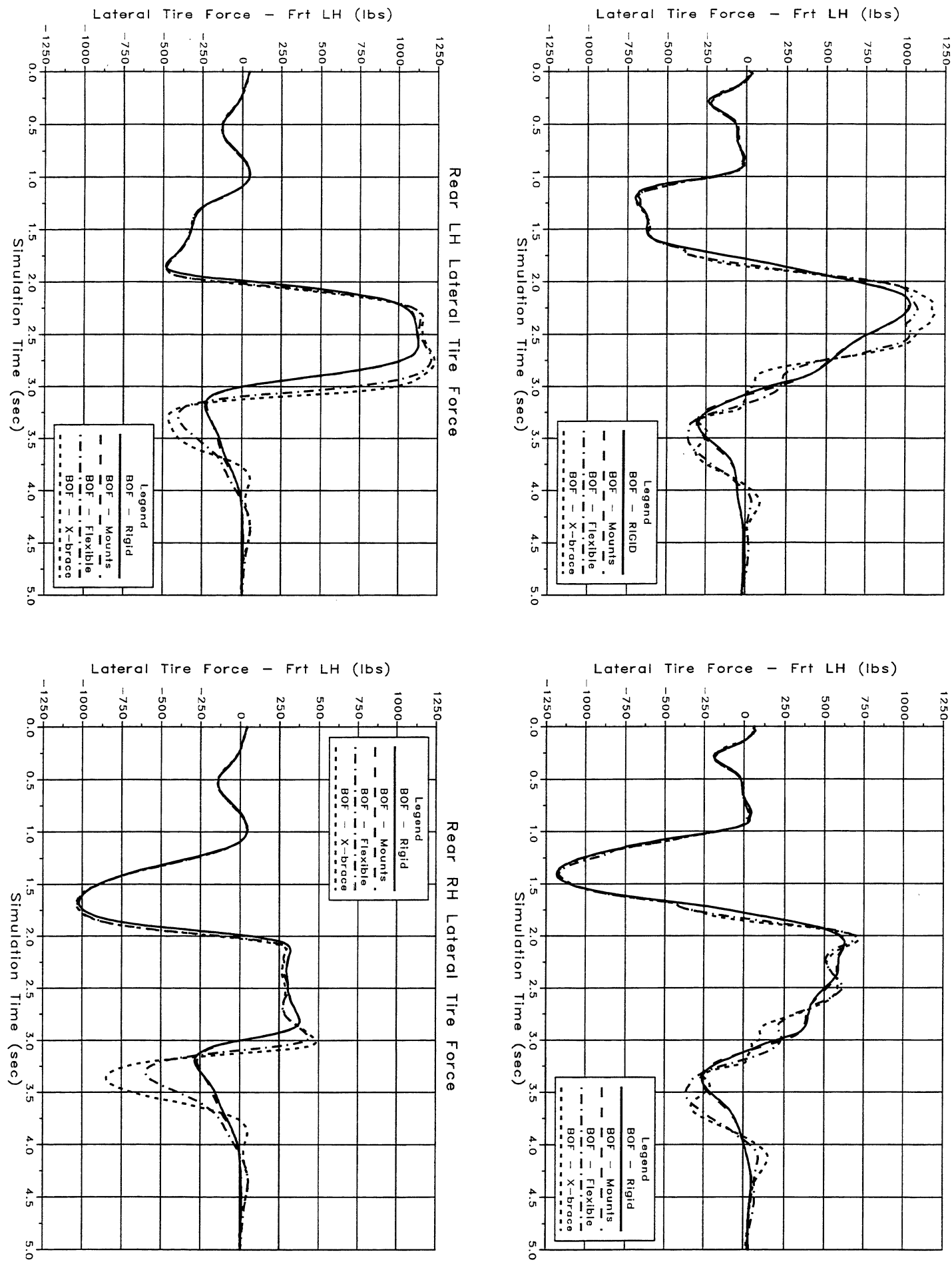

Fig. 18 Lane Change Comparison -- All 4 Models -- Tire Lateral Forces

Discussion

Results from the lane change maneuver indicate the structural compliance of the vehicle frame has a significant influence on the transient handling performance, as expected. This influence is very apparent in the later portion of the lane change maneuver as the vehicle transitions from one extreme loading condition to the other. The vehicle requires more steering wheel input to negotiate the lane change and more correction (over shoot) is required to exit the lane change. Random steer results indicate that body mount compliance influence vehicle dynamics more than frame compliance at lower levels of lateral accelerations (<0.35g). This is indicated by the lack of change of the BOF-Mount and the BOF-Flexible configurations between the 0.2g and 0.35g events. The BOF-Rigid configuration displays a reduction in yaw and lateral acceleration frequency response consistent with an understeering vehicle.

The lane change results, in conjunction with animation, indicate that the majority of the structural compliance influencing vehicle handling is occurring near the rear axle. Plan view "match boxing" combined with torsional deflection delay the lateral tire force reduction on the rear axle (see lateral tire force plots). The vehicle develops more yaw angle as a result of this increased application of side force, requiring more steer angle from the front axle to maintain the vehicle on the specified path (see tire slip angle plots). The addition of the X-brace, meant to reduce plan view "match boxing", seems to amplify this phenomenon. It is speculated that the X-brace places more load in the area of unwanted compliance, accentuating the tire side force delay. This is further evidence that the majority of the structural compliance influencing vehicle handling is occurring near the rear axle.

Conclusions

Results from this analysis have provided valuable insight as to why modifications made to the front suspension, in an attempt to improve vehicle dynamics, were not fully realized. Also, it would tend to indicate that improvements to the rear suspension system lateral stiffness, including supporting structure, are required to "balance" the vehicle and improve handling response.

In general, whenever the structural flexibility of system components appreciably effects the motion history of the system, that flexibility must be included in the system modeling. For structures such as the frame in this example where the structural mass idealization is simplified by the system configuration, the discrete idealization is quite capable of capturing frequency as well as compliance effects. More complex structures, such as vehicle bodies, will, in general, require more detailed mass modeling, such as that associated with the modal elastic approach now coming into use with the latest versions of ADAMS.

Bibliography

1) Modeling Compliant Vehicle Structures at Ford Chassis Systems Using the ADAMS MSS Software -- Case Study: FN74, (Ford internal Report), McConville, J. B., Ford, Dearborn, MI, '93.

2) ADAMS/Finite Element Reference Manual, Version 7.1, anon., Mechanical Dynamics, Inc., Ann Arbor MI, '94.

3) ADAMS/Linear Option, Version 8.0, anon., Mechanical Dynamics, Inc., Ann Arbor MI, '94.

4) Vehicle Dynamics Guide, anon., Ford Engineering Test Services, Ford Motor Company Dearborn MI, '93.